Clinical Science (2023) **137** 317–331
https://doi.org/10.1042/CS20220537

PORTLAND PRESS

Research Article

The long noncoding RNA Meg3 mediates TLR4-induced inflammation in experimental obstructive nephropathy

Wai Han Yiu[1], Sarah W.Y. Lok[1], Rui Xue[1], Jiaoyi Chen[1], Kar Neng Lai[1], Hui Yao Lan[2] and Sydney C.W. Tang[1]

[1]Department of Medicine, The University of Hong Kong, Queen Mary Hospital, Hong Kong; [2]Department of Medicine and Therapeutics and Li Ka Shing Institute of Health Sciences, The Chinese University of Hong Kong, Hong Kong

Correspondence: Sydney C.W. Tang (scwtang@hku.hk)

Kidney inflammation contributes to the progression of chronic kidney disease (CKD). Modulation of Toll-like receptor 4 (TLR4) signaling is a potential therapeutic strategy for this pathology, but the regulatory mechanisms of TLR4 signaling in kidney tubular inflammation remains unclear. Here, we demonstrated that tubule-specific deletion of TLR4 in mice conferred protection against obstruction-induced kidney injury, with reduction in inflammatory cytokine production, macrophage infiltration and kidney fibrosis. Transcriptome analysis revealed a marked down-regulation of long noncoding RNA (lncRNA) Meg3 in the obstructed kidney from tubule-specific TLR4 knockout mice compared with wild-type control. Meg3 was also induced by lipopolysaccharide in tubular epithelial cells via a p53-dependent signaling pathway. Silencing of Meg3 suppressed LPS-induced cytokine production of CCL-2 and CXCL-2 and the activation of p38 MAPK pathway *in vitro* and ameliorated kidney fibrosis in mice with obstructive nephropathy. Together, these findings identify a proinflammatory role of lncRNA Meg3 in CKD and suggest a novel regulatory pathway in TLR4-driven inflammatory responses in tubular epithelial cells.

Introduction

Inflammation is one of the common pathogenic mechanisms in many kidney diseases including ischemia–reperfusion injury (IRI), immune-mediated nephritis, allograft rejection and diabetic nephropathy (DN) in which immune cells interact with intrinsic renal cells in response to either pathogens or endogenous danger signals, leading to tissue damage and kidney failure [1]. Toll-like receptors (TLRs) are well known to be involved in the recognition of pathogen-associated molecular patterns (PAMPs) and damage-associated molecular patterns (DAMPs). Activation of TLRs triggers various signaling cascades to activate transcription factor-regulated inflammatory responses, resulting in cytokine and chemokine production, leukocyte infiltration and progressive fibrosis [2].

Among the TLR family, TLR4 has been identified as a key mediator in kidney inflammation and progressive kidney fibrosis [3]. Overexpression of TLR4 in mice with gp96 on cell surface induced lupus-like glomerulonephritis without external injury [4]. TLR4 signaling mediated ischemia–reperfusion injury and was associated with renal allograft rejection after kidney transplantation. Improved graft function with decreased inflammatory responses were observed from patients who received a donor kidney with missense mutations in TLR4 [5]. Mice deficient in TLR4 were protected against renal IRI, accompanied by the reduction of proinflammatory cytokine and chemokine production, leukocyte infiltration and tubular cell apoptosis [6]. Apart from participating in acute inflammation, accumulating evidence show that the activation of TLR4 is involved in the pathogenesis of kidney fibrosis during progressive chronic kidney disease (CKD). The expression of TLR4 was up-regulated in the glomeruli and tubules of patients with

Received: 16 August 2022
Revised: 25 January 2023
Accepted: 27 January 2023

Accepted Manuscript online: 27 January 2023
Version of Record published: 01 March 2023

Clinical Science (2023) **137** 317–331
https://doi.org/10.1042/CS20220537

DN [7]. Tubular TLR4 overexpression correlated with macrophage infiltration in the diabetic kidney and TLR4 expression was also increased in neutrophils and monocytes from CKD patients, suggesting a role of TLR4 in mediating kidney inflammation in CKD [8,9]. Thus, TLR4 signaling is a promising therapeutic target in inflammatory kidney diseases. TLR4 is widely expressed in both myeloid cells and resident renal cells of the kidney including tubular epithelial cells, mesangial cells, podocytes and endothelial cells [10], thus understanding the cell type-specific regulatory mechanisms of TLR4 signaling may advance understanding of the pathogenesis of inflammatory kidney diseases and provide new insights for precision medicine in the future.

Increasing evidence show that long noncoding RNAs (lncRNAs) are implicated in the pathogenesis of many diseases such as rheumatoid arthritis, cardiovascular disease and diabetes [11–13]. In the context of kidney disease, lncRNAs have been reported to participate in kidney fibrosis [14]. Erbb4-IR is a Smad3-related lncRNA that regulates collagen 1 and α-SMA transcription via inhibiting Smad7 [15]. Other lncRNAs including lnc-ARAP1-AS2 and lnc-ATB are involved in epithelial–mesenchymal transition (EMT) [16,17]. In recent years, lncRNAs have emerged as a critical player in innate immunity [18]. For example, Lnc-MC and LincRNA-Cox2 are involved in macrophage differentiation and polarization and lnc-DC regulates dendritic cell maturation [19–21]. By altering chromatin structure, gene transcription and protein modification, lncRNAs modulate inflammatory responses [22]. Given the importance of TLR4 in evoking inflammatory responses in kidney disease, understanding the role of lncRNA in the activation of TLR4 signaling may unravel more effective therapeutic strategies in combating kidney inflammation.

Here, we demonstrated a pathogenetic role of TLR4 signaling in kidney tubules by using tubule-specific TLR4 knockout (KO) mice in the experimental model of obstructive nephropathy through which maternally expressed gene 3 (Meg3) was identified as a TLR4-dependent lncRNA. Our results showed that Meg3 was induced by lipopolysaccharide (LPS) via TLR4/p53 signaling. Knockdown of Meg3 in tubular epithelial cells suppressed LPS-induced inflammatory cytokine production. This is mirrored in animals in which kidney-specific silencing of Meg3 protected against kidney fibrosis. Therefore, targeting Meg3 may be a promising novel approach to regulate kidney tubular inflammation and fibrosis.

Methods

Experimental model of unilateral ureteral obstruction (UUO)

All work with animals were approved by the Committee on the Use of Live Animals in Teaching and Research of the University of Hong Kong and was performed in accordance with the NIH Guide for the Care and Use of Laboratory Animal. All animal works were conducted in the Centre for Comparative Medicine Research (CCMR) at the University of Hong Kong.

The conditional KO mice (Ksp-TLR4$^{f/f}$) in which TLR4 gene was specifically deleted in renal tubular epithelial cells were generated by crossing homozygous TLR4 floxed mice (TLR4$^{f/f}$ with C57BL/6J background) (Stock #024872) with kidney-specific Ksp-Cre transgenic mice (C57BL/6J background) (Stock#012237) from Jackson Laboratory; Bar Habor, ME. Age and sex-matched TLR4$^{f/f}$ were used as control. Genotyping of ear biopsy samples from mice were confirmed by PCR method using the following primers; Cre transgene, 5′-GCA GAT CTG GCT CTC CAA AG-3′ and 5′-AGG CAA ATT TTG GTG TAC GG-3′ and TLR4 floxed alleles, 5′-TGA TGG TGT GAG CAG GAG AG-3′ and 5′-TGA CCA CCC ATA TTG CCT ATA C-3′. At the age of 8 weeks, male Ksp-TLR4$^{f/f}$ (n=7) and TLR4$^{f/f}$ (n=7) mice were subjected to the surgery of UUO on the left kidney according to established procedures [23]. Sham operation was performed on control mice (n=7) with abdominal cavity incision only. Mice were anesthetized with ketamine, xylazine, and acepromazine mixture (100 mg/kg + 10 mg/kg + 3 mg/kg; intraperitoneal injection) for the surgical procedures. All mice were killed at day 7 after UUO with injection of pentobarbital (150 mg/kg; I.P.) after experiment. Blood and kidneys were collected for further analyses.

Ultrasound-mediated gene transfer of Meg3 knockdown in UUO mice

Prior to the surgery of UUO, shRNA-pSuper.puro vector targeting Meg3 (200 μg/mouse) (n=7) or pSuper.puro empty vector (OligoEngine, Seattle, WA, U.S.A.) (n=7) was transfected into the left kidney of male C57BL/6J mice as described previously [24]. Briefly, shRNA vector was mixed with Sonovue microbubbles (Bracco, Milan, Italy) at a ratio of 1:1 (vol:vol) and injected into mice via the tail vein. An ultrasound transducer (Therasonic, Electro Medical Supplies, Wantage, U.K.) was immediately applied on the skin of the back against the left kidney with a pulse-wave output of 1 MHz at 2 W/cm^2 for 5 min. All mice were sacrificed at day 7 after UUO with injection of pentobarbital (150 mg/kg; I.P.) after experiment. Blood and kidneys were collected for further analyses.

Histological and immunohistochemical staining

Kidneys were fixed in 10% neutral-buffered formalin and paraffin-embedded. Tissue sections (4 μm) were subjected to periodic acid–Schiff (PAS) and Masson's Trichrome Staining (Sigma–Aldrich, St Louis, MO, U.S.A.) by standard protocol. Histological changes of the renal cortex were evaluated according to the severity of tubular dilatation, atrophy, and cast formation using a semiquantitative scoring system from 0 to 5, as previously described [25]. Histological analysis was performed in a blind manner. Immunohistochemical staining was performed on paraffin-embedded kidney sections according to the established protocol [25]. The primary antibodies against F4/80 (Serotec, Oxford, U.K.), Col-3 (Southern Biotech, Birmingham, AL, U.S.A.), and α-SMA (Sigma-Aldrich) were used, followed by peroxidase conjugated secondary antibodies. The immunocomplex were visualized using DAB substrate from Envision Plus system (Dako, Carpinteria, CA, U.S.A.). All sections were counterstained with hematoxylin before mounting. The number of positive cells for F4/80 from 20 different fields were counted under high-power field (400× magnification). The percentage of positive staining of kidney sections was quantified by Image J software (NIH, Bethesda, MD, U.S.A.).

RNA-sequencing and bioinformatics analysis

The UUO kidney was perfused with PBS and harvested for the RNA extraction using NucleoSpin RNA kit (Macherey-Negel, Düren, Germany). RNA integrity was assessed by Agilent 2100 Bioanalyzer (Agilent Technologies, Palo Alto, CA, U.S.A). A total amount of 1 μg RNA was used as input for ribosomal RNA depletion using Ribo-Zero Gold rRNA Removal Kit (Illumina, San Diego, CA, U.S.A.). After that, the residual RNA was used for library construction using KAPA Stranded RNA-Seq Kit (Illumina). Pair-End 101bp sequencing was performed on HiSeq 1500 platform (Illumina). The library preparation and sequencing were performed by Centre for PanorOmic Sciences at the University of Hong Kong. Raw reads were processed by FastQC to remove low quality reads and adaptors (http://www.bioinformatics.babraham.ac.uk/projects/fastqc/). Clean reads were aligned to mouse reference genome (Ensembl GRCm38.75) using STAR and assembled with Cufflinks. Transcript abundances were quantified by RSEM. Differentially expressed gene (DEG) analysis was performed by DESeq2 to detect a significant difference ($P<0.05$). Gene Ontology (GO) and Kyoto Encyclopedia of Genes and Genomes (KEGG) pathways were analyzed to identify the functional enrichment of DEGs.

Cell culture, LPS treatment and transfection

Mouse kidney tubular epithelial cells (C1.1) were cultured in Dulbecco's modified Eagle medium/nutrient mixture F12, supplemented with 100 IU/ml penicillin, 100 μg/ml streptomycin, and 10% fetal bovine serum (Invitrogen, Carlsbad, CA, U.S.A.) at 37°C in 5% carbon dioxide atmosphere. Confluent, growth arrested cells were incubated with medium containing 0.01–5 mg/ml lipopolysaccharide (LPS) for different times (1–3 h). To investigate the signaling pathways involved, cells were pretreated for 1 h with 3 μM CLI-095, 20 μM SB203580, 20 μM PD98059, 2 μM Bay11-7085, 20 μM pifithrin-α, and 10 μM RITA prior to LPS stimulation. To knockdown Meg3, cells were transfected with siRNA-Meg3 or scrambled siRNA using Lipofectamine® 2000 reagent (Invitrogen).

In situ hybridization

In situ hybridization was performed on paraffin-embedded kidney sections (4 μm) using RNAscope®2.5 HD Duplex Detection Kit (Chromogenic) according to the manufacturer's instructions (Advanced Cell Diagnostics, Newark, CA, U.S.A.). Briefly, deparaffinized and rehydrated tissue sections were quenched with H_2O_2, followed by antigen retrieval and protease pretreatment. Tissue sections were then hybridized simultaneously with RNAscope probe for Mm-TLR4 (#316801-C2) and Mm-Meg3 (#527201) for 2 h. The positive signals were amplified and detected by horseradish peroxidase-based cyan and alkaline phosphatase-based red chromogenic substrates. Sections were counterstained with hematoxylin and mounted.

RNA extraction and real-time qPCR analysis

Total RNAs were extracted from renal cortical tissue or cultured cells and reverse transcribed into cDNA as described previously [25]. Real-time qPCR was performed using SYBR™ Green reagent and specific primers on the StepOnePlus™ Real-Time PCR System (Applied Biosystems, Carlsbad, CA, U.S.A.). Relative gene expression was obtained after normalization with GAPDH, followed by the comparison with respective control group using StepOne™ software v2.3 (Applied Biosystems). Sequence of primers were listed in Table 1.

Clinical Science (2023) **137** 317–331
https://doi.org/10.1042/CS20220537

Table 1 Primer sequences for real-time qPCR

Gene	Forward primer 5′ → 3′	Reverse primer 5′ → 3′
Meg3 (mouse)	GGACTTCACGCACAACACGTT	GTCCCACGCAGGATTCCA
H-19 (mouse)	GAACAGAAGCATTCTAGGCTG	TTCTAAGTGAATTACGGTGGG
Rian (mouse)	ATGTCTGCTGCCCTGTCGTCT	GCGGTCACTGCCAAGGTCTCT
TLR4-Ex3 (mouse)	CATCCAGGAAGGCTTCCACA	GGCGATACAATTCCACCTGC
CCL-2 (mouse)	CTCTTCCTCCACCACCAT	CTCTCCAGCCTACTCATTG
CXCL-2 (mouse)	CGGTCAAAAAGTTTGCCTTG	TCCAGGTCAGTTAGCCTTGC
TNF-α (mouse)	CCGATGGGTTGTACCTTGTC	GGCAGAGAGGAGGTTGACTTT
GAPDH (mouse)	GCACAGTCAAGGCCGAGAAT	GCCTTCTCCATGGTGGTGAA

Western blot analysis

Total proteins were prepared from cortical kidney tissue or cultured cells using RIPA lysis buffer (Millipore, Bedford, MA, U.S.A.). Equal amount of proteins were resolved in 4–12% SDS-PAGE gel (Invitrogen), transferred to a PVDF membrane (Millipore). After blocking, membrane was incubated overnight with primary antibodies against fibronectin (Sigma), KIM-1 (R&D Systems, Minneapolis, MN, U.S.A.), TLR4 (Santa Cruz Biotechnology, Santa Cruz, CA, U.S.A.), p-IκB, total IκB, p-p38, and p38 (Cell Signaling Technology, Beverly, MA, U.S.A.). The immunocomplex was visualized with ECL prime chemiluminescence (Bio-Rad, Hercules, CA, U.S.A.) using the ChemiDoc XRS system (Bio-Rad). Quantification of protein bands was performed by the ImageJ program (NIH) and was normalized to GAPDH level.

Renal function

Serum creatinine and BUN levels were determined by the commercial kits (Stanbio Laboratory, Boerne, TX, U.S.A.).

ELISA

Renal cortical tissues were homogenized in T-PER™ tissue protein extraction reagent (Thermo Scientific, Waltham, MA, U.S.A.) and centrifuged to obtain tissue lysates. Protein concentration was determined by Pierce™ BCA protein assay kit (Thermo Scientific). Culture supernatant was collected after treatment. The level of CCL-2 and CXCL-2 from tissue lysates and culture supernatant were quantified by commercial kits (R&D Systems, Minneapolis, MN, U.S.A.) according to the manufacturer's instructions.

Statistical analysis

All data were obtained from at least three independent experiments and expressed as mean ± SEM. Differences between multiple groups were evaluated with one-way analysis of variance followed by Bonferroni's comparison using GraphPad Prism (GraphPad Software, San Diego, CA, U.S.A.). Data were considered statistically significant at $P<0.05$ ($^{*}P< 0.05$; $^{**}P<0.01$, and $^{***}P<0.001$).

Results

Tubule-specific deletion of TLR4 ameliorates kidney fibrosis

To determine how TLR4 in tubule cells contributes to kidney fibrosis, the floxed TLR4 mice ($TLR4^{f/f}$) were mated with Ksp-Cre mice which express Cre recombinase under the cadherin 16 promoter to generate conditional tubule-specific TLR4 KO mice (Ksp-$TLR4^{f/f}$) (Figure 1A). Ksp-$TLR4^{f/f}$ mice were born at the expected Mendelian frequency. At day 7 after UUO, Ksp-$TLR4^{f/f}$ mice showed significant deletion of TLR4 in the whole kidney by real-time PCR (Figure 1B) and Western blotting (Figure 1C), compared with $TLR4^{f/f}$ mice. We next examined whether ablation of tubular TLR4 affected kidney inflammatory and fibrotic responses after obstructive injury. As shown by PAS staining, Ksp-$TLR4^{f/f}$ UUO mice exhibited significant improvement in kidney histology compared with $TLR4^{f/f}$ mice (Figure 2A). The expressions of Col-3 and α-SMA were reduced in Ksp-$TLR4^{f/f}$ mice. Masson's Trichrome staining demonstrated that tubulointerstitial fibrosis was significantly increased in the UUO kidney from $TLR4^{f/f}$ mice but reduced in that of Ksp-$TLR4^{f/f}$ mice (Figure 2B). Western blot analyses also revealed a reduction of fibronectin in UUO kidneys of Ksp-$TLR4^{f/f}$ mice compared with $TLR4^{f/f}$ mice. Increased levels of KIM-1 in UUO kidneys of $TLR4^{f/f}$ mice were significantly suppressed in Ksp-$TLR4^{f/f}$ mice (Figure 2C).

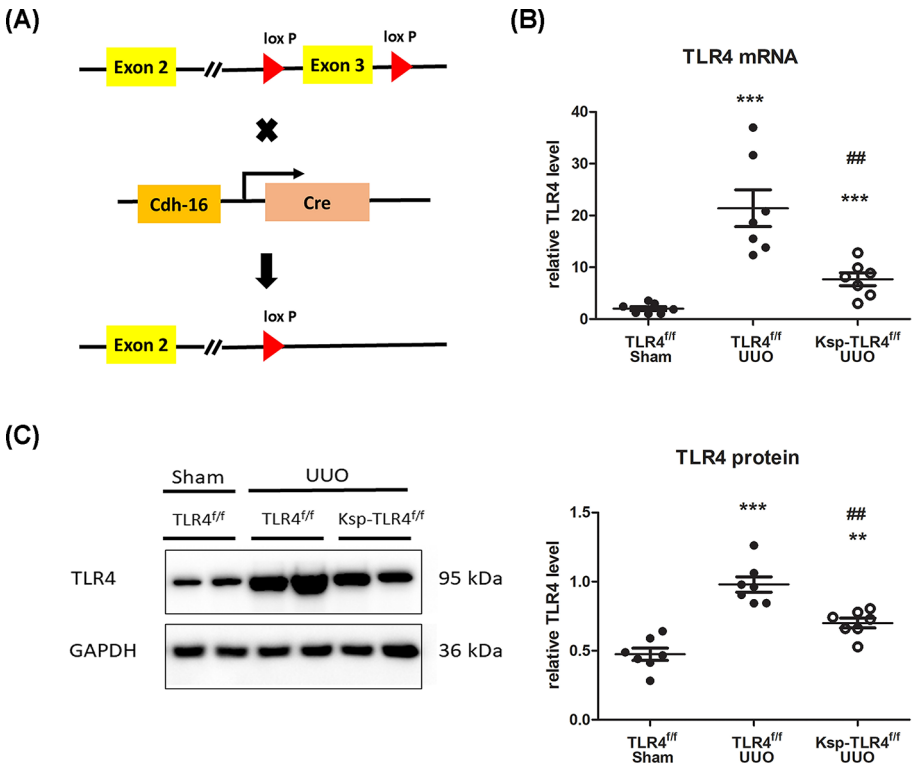

Figure 1. Generation of tubule-specific deletion of TLR4 in mice

(**A**) Schematic illustration of breeding strategy for generating Ksp-TLR4$^{f/f}$ mice. (**B**) TLR4 mRNA expression determined by real-time qPCR in TLR4$^{f/f}$ sham mice, TLR4$^{f/f}$ UUO mice, and Ksp-TLR4$^{f/f}$ UUO mice. (**C**) TLR4 protein expression determined by Western blot analysis. $^{***}P<0.001$ and $^{**}P<0.01$ vs. TLR4$^{f/f}$ sham mice; $^{\#\#}P<0.01$ vs. TLR4$^{f/f}$ UUO mice ($n=7$ in each group).

Deletion of tubular TLR4 protects against kidney inflammation

Following UUO, injured cells release DAMPs that lead to sterile inflammation. TLR4$^{f/f}$ mice showed a significant increase in mRNA and protein expression of CCL-2, CXCL-2, and TNF-α in UUO kidneys, which were suppressed in Ksp-TLR4$^{f/f}$ mice (Figure 3A). Kidney inflammation was accompanied by a markedly increase in the number of infiltrating macrophages (F4/80^{+} cells) in TLR4$^{f/f}$ mice, whereas Ksp-TLR4$^{f/f}$ mice showed less macrophage infiltration in the UUO kidneys (Figure 3B). UUO-induced kidney inflammation was associated with activation of NF-κB signaling, as evidenced by an increase in phosphorylated IκB in kidney tissues of TLR4$^{f/f}$ mice which was inhibited in Ksp-TLR4$^{f/f}$ mice (Figure 3C). Moreover, tubule-specific deletion of TLR4 could improve renal function of UUO mice as shown by a reduction in BUN and serum creatinine levels compared with TLR4$^{f/f}$ mice (Figure 3D).

Down-regulation of lncRNA Meg3 in the obstructed kidneys from tubule-specific TLR4 KO mice

To uncover the mechanism underlying the renoprotective effects and identify the change of lncRNAs associated with the ablation of tubule-specific TLR4 during UUO, whole transcriptome sequencing (RNA-seq) was performed in UUO kidneys from TLR4$^{f/f}$ mice ($n=2$) and Ksp-TLR4$^{f/f}$ mice ($n=2$). About 58–66 million clean reads were obtained from each sample which contained more than 70% reads mapped to the reference genome. A total of 836 significant DEGs ($P<0.05$, log2FoldChange ≥ 0.5 or ≤ -0.5) were identified from kidney tissues of UUO kidneys in TLR4$^{f/f}$ and Ksp-TLR4$^{f/f}$ mice. Among these significant DEGs, 593 were down-regulated and 243 were up-regulated in UUO kidneys from Ksp-TLR4$^{f/f}$ mice compared with TLR4$^{f/f}$ mice (Figure 4A). The GO and KEGG pathway analysis of DEGs ($P<0.05$) revealed that those down-regulated genes in Ksp-TLR4$^{f/f}$ mice were enriched in leukocyte aggregation (GO:0070486), regulation of non-canonical Wnt signaling (GO:2000050), negative regulation of cell proliferation (GO:0008285) and Smad protein signaling (GO:0060395). Conversely, those up-regulated genes in Ksp-TLR4$^{f/f}$ mice were involved in kidney physiologic functions including monovalent inorganic cation homeostasis (GO:0055067), ion transport (GO: R-MMU-983712, GO:0043269 and GO:0006820) (Figure 4B).

Clinical Science (2023) **137** 317–331
https://doi.org/10.1042/CS20220537

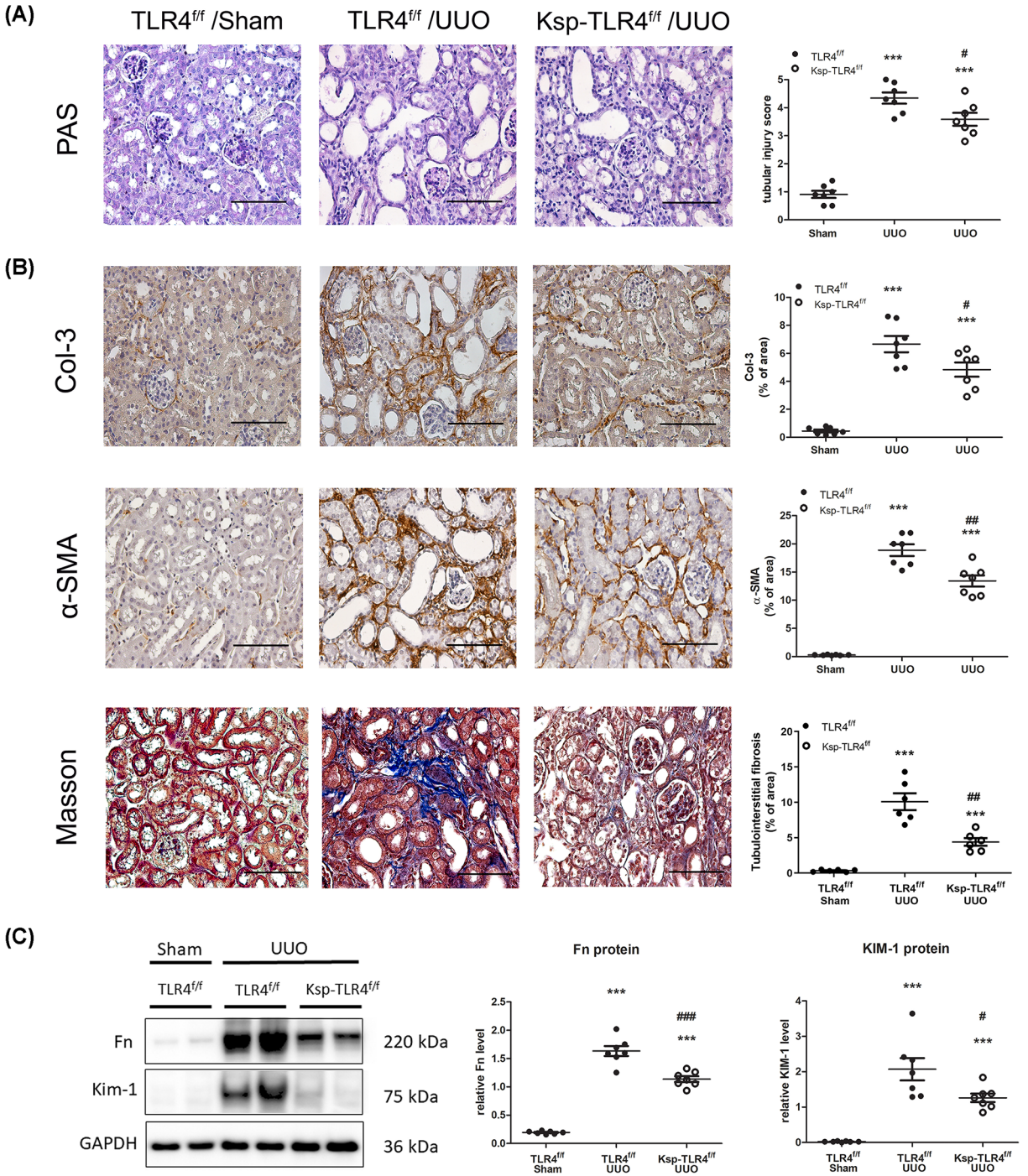

Figure 2. Deletion of tubular TLR4 ameliorates kidney fibrosis

(**A**) Representative PAS staining of renal tissues in TLR4$^{f/f}$ sham mice, TLR4$^{f/f}$ UUO mice and Ksp-TLR4$^{f/f}$ UUO mice and quantitative analysis. Bar = 100 μm. (**B**) Representative immunohistochemical staining of Col-3, α-SMA and Masson's Trichrome staining in different groups and the corresponding quantitative analysis; bar = 100 μm. (**C**) Western blotting analyses shows renal expression of Fn and KIM-1 in different groups and the corresponding quantitative analysis. $^{***}P<0.001$ vs. TLR4$^{f/f}$ sham mice; $^{###}P<0.001$, $^{##}P<0.01$ and $^{#}P<0.05$ vs. TLR4$^{f/f}$ UUO mice ($n=7$ in each group).

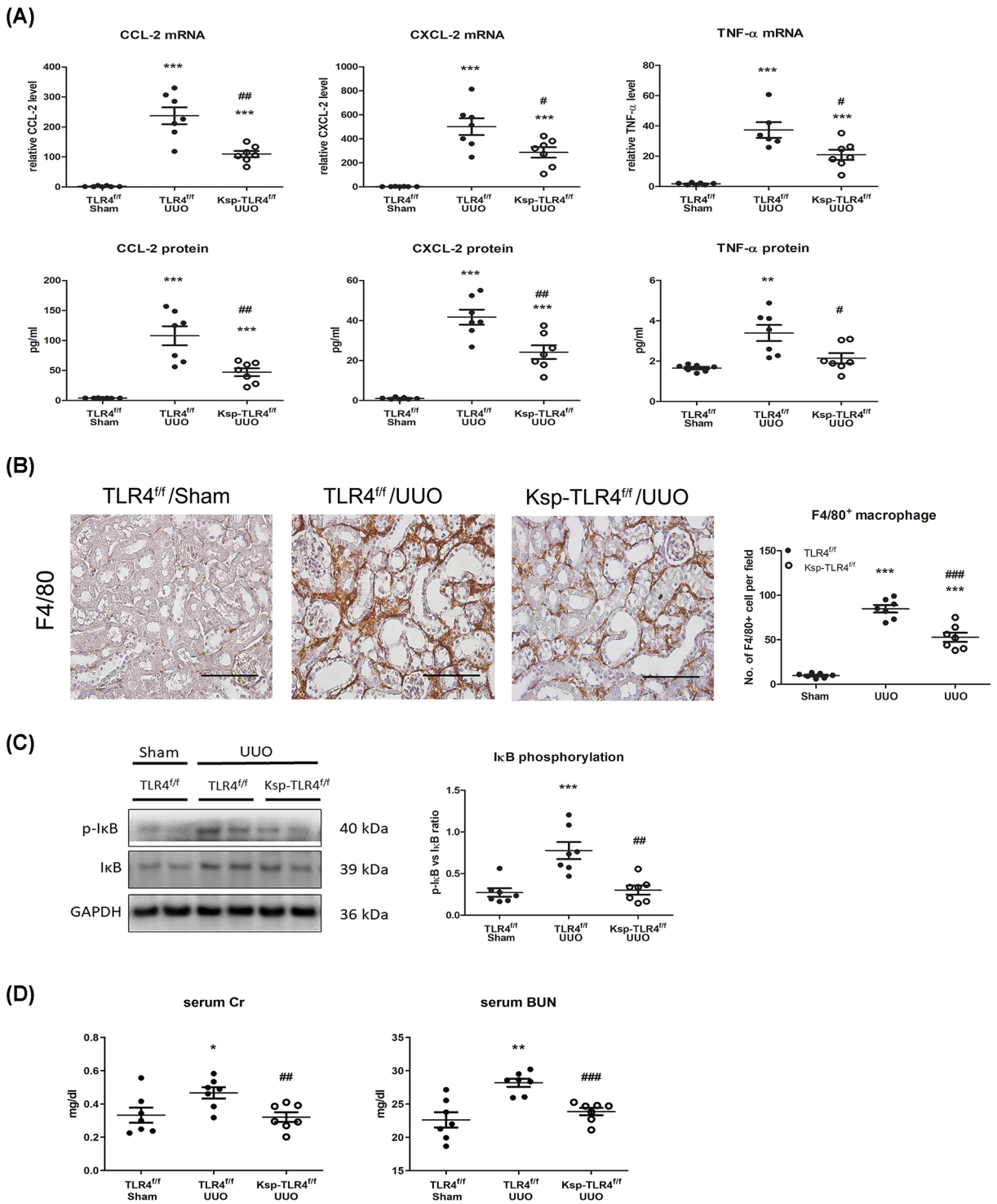

Figure 3. Deletion of tubular TLR4 reduces renal inflammation

(**A**) Quantitative real-time PCR shows relative mRNA and protein expression levels of CCL-2, CXCL-2, and TNF-α in renal tissues from TLR4$^{f/f}$ sham mice, TLR4$^{f/f}$ UUO mice and Ksp-TLR4$^{f/f}$ UUO mice. (**B**) Representative immunohistochemical staining of F4/80 in different groups and the corresponding quantitative analysis. Bar = 100 μm (**C**) Western blotting analyses shows phosphorylation level of IκB and total IκB in different groups and the corresponding quantitative analysis. (**D**) Serum creatinine (Cr) and blood urea nitrogen (BUN) levels in different groups. $^{***}P<0.001$, $^{**}P<0.01$, and $^{*}P<0.05$ vs. TLR4$^{f/f}$ sham mice; $^{###}P<0.001$, $^{##}P<0.01$, and $^{#}P<0.05$ vs. TLR4$^{f/f}$ UUO mice (n=7 in each group).

Clinical Science (2023) **137** 317–331
https://doi.org/10.1042/CS20220537

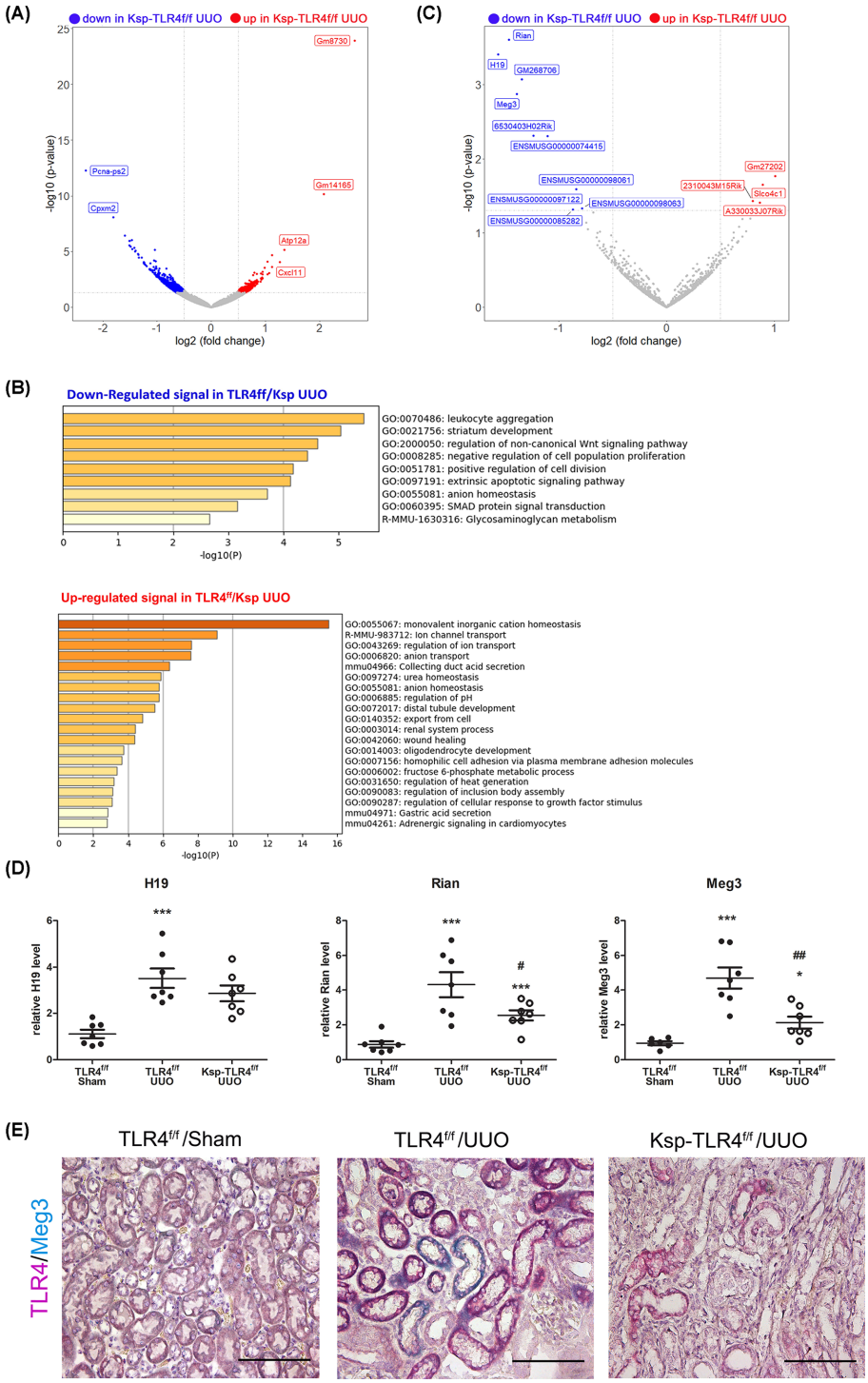

Figure 4. RNA sequencing reveals differentially expressed genes (DEGs) between TLR4$^{f/f}$ UUO mice and Ksp-TLR4$^{f/f}$ UUO mice

(**A**) The volcano plot of transcriptomic changes between renal tissues from TLR4$^{f/f}$ UUO mice and Ksp-TLR4$^{f/f}$ UUO mice. (**B**) Enrichment analysis of DEGs that were down-regulated and up-regulated in Ksp-TLR4$^{f/f}$ UUO mice vs. TLR4$^{f/f}$ UUO mice. (**C**) The volcano plot of lncRNA changes between renal tissues from TLR4$^{f/f}$ UUO mice and Ksp-TLR4$^{f/f}$ UUO mice. (**D**) Quantitative real-time PCR shows relative expression levels of H-19, Rian, and Meg3 in renal tissues in different groups and the corresponding quantitative analysis. (**E**) *In situ* hybridization of Meg3 and TLR4 expression in kidney tissue from different groups. Red color indicated positive signal for TLR4 and cyan color indicated positive signal for Meg3. $^{***}P<0.001$ and $^{*}P<0.05$ vs. TLR4$^{f/f}$ sham mice; $^{\#\#}P<0.01$ and $^{\#}P<0.05$ vs. TLR4$^{f/f}$ UUO mice.

We next examined the differential expression of lncRNAs between UUO kidneys from $TLR4^{f/f}$ mice and Ksp-$TLR4^{f/f}$ mice. In total, 14 lncRNAs were significantly differentially expressed, of which 10 were down-regulated and 4 were up-regulated in Ksp-$TLR4^{f/f}$ mice compared with $TLR4^{f/f}$ mice (Figure 4C). We selected the top 3 differentially expressed lncRNAs (H19, Rian, and Meg3) for experimental validation by real-time PCR analysis. Although all of them were significantly up-regulated in UUO kidneys of $TLR4^{f/f}$ mice, which were suppressed from those of Ksp-$TLR4^{f/f}$ mice, the expression level of Meg3 showed the most significant down-regulation in tubule-specific TLR4 KO mice (Figure 4D). Consistent with this finding, the transcript levels of TLR4 and Meg3 were markedly induced and partially co-localized in UUO kidney from $TLR4^{f/f}$ mice, but their expression levels were significantly reduced in UUO kidney from Ksp-$TLR4^{f/f}$ mice as determined by *in situ* hybridization (Figure 4E).

LncRNA Meg3 is involved TLR4-mediated inflammatory responses in tubular cells

Given that Meg3 was induced in wild type and down-regulated in tubule-specific TLR4 KO UUO kidneys, we next investigated the correlation between TLR4 signaling and Meg3 in cultured tubular epithelial cells by stimulating with LPS, a TLR4 ligand. As shown in Figure 5A, the expression of Meg3 was induced by LPS in a time- and dose-dependent manner, which peaked at 3 h at a concentration of 1 μg/ml, whereas LPS-induced Meg3 expression was inhibited by the pretreatment with CLI-095, a TLR4 inhibitor. The upstream mediator of Meg3 expression upon activation of TLR4 signaling was further elucidated using pharmacological inhibitors. Pretreatment with SB203580 (p38), PD98059 (MEK) and Bay11-7085 (NF-κB) did not affect LPS-induced up-regulation of Meg3 (Figure 5B). However, the expression of LPS-induced Meg3 was significantly abrogated by inhibiting p53 signaling with pifithrin-α (PFT-α), whereas Meg3 expression was markedly induced by activating p53 with RITA (Figure 5C). These results indicate that LPS-induced Meg3 expression in tubular epithelial cells is regulated by the p53 pathway.

Since Meg3 was shown to be the downstream target of TLR4 signaling, we hypothesized that Meg3 might exert a functional role in TLR4-mediated inflammatory process. To this end, LPS-induced Meg3 expression was depleted by siRNA (Figure 5D). Knockdown of Meg3 significantly inhibited LPS-induced expression of CCL-2 and CXCL-2 (Figure 5E) and suppressed the phosphorylation of p38 MAPK protein (Figure 5F).

Gene silencing of Meg3 attenuates kidney fibrosis in UUO mice

Meg3 expression was progressively induced in the model of UUO (Figure 6A). To determine the functional role of Meg3 in kidney inflammation and fibrosis *in vivo*, we knocked down Meg3 by delivering shRNA expressing vector into the kidney using ultrasound microbubble-mediated gene transfer (Figure 6B). Real-time PCR showed that Meg3 expression was markedly increased at 7 days after UUO and was significantly suppressed after Meg3 shRNA plasmid injection (Figure 6C). UUO mice treated with Meg3 shRNA showed improved kidney histology with a reduction of tubular dilation and atrophy (Figure 7A). Masson's Trichrome staining showed less tubulointerstitial fibrosis with reduced expression Col-3, α-SMA (Figure 7B), and macrophage infiltration (Figure 7C) compared with UUO mice treated with vehicle.

Discussion

Inflammation is a key wound healing process during kidney injury; however, it is also a contributor to fibrogenic responses [26]. Increasing evidence shows that kidney fibrosis associates with the activation of TLR4 signaling that leads to the induction of inflammatory cytokines. Mice with global deletion of TLR4 exhibited reduction in interstitial fibrosis in response to UUO [27] and demonstrated the improvement in kidney inflammation in the streptozotocin-induced diabetic model [8,28]. Here, we investigated the regulatory mechanisms of TLR4 signaling in tubulointerstitial inflammation by generating a conditional tubule-specific TLR4 KO mouse and identifying the functional role of TLR4-related lncRNA Meg3 in both UUO mice and cultured tubular epithelial cells. Our tubule-specific TLR4 KO mice showed a significant reduction of TLR4 expression in UUO kidney while its expression was slightly decreased at the Sham group (Supplementary Figure S1), indicating a profound up-regulation of tubular TLR4 expression in response to injury. Tubule-specific TLR4 KO mice showed less obstruction-induced tubular damage, kidney inflammation and interstitial fibrosis than wild-type mice, and improvement of renal function in UUO mice. Transcriptome analysis also revealed that deletion of tubular TLR4 suppressed genes associated with profibrotic pathways including Smad and Wnt signaling pathways. In particular, Meg3 was identified for the first time to be the pro-inflammatory mediator of TLR4 signaling in both UUO mice and tubular cells. Blockade of Meg3 ameliorated kidney injury in UUO mice, suggesting an attractive therapeutic target for kidney inflammation and fibrosis.

Clinical Science (2023) **137** 317–331
https://doi.org/10.1042/CS20220537

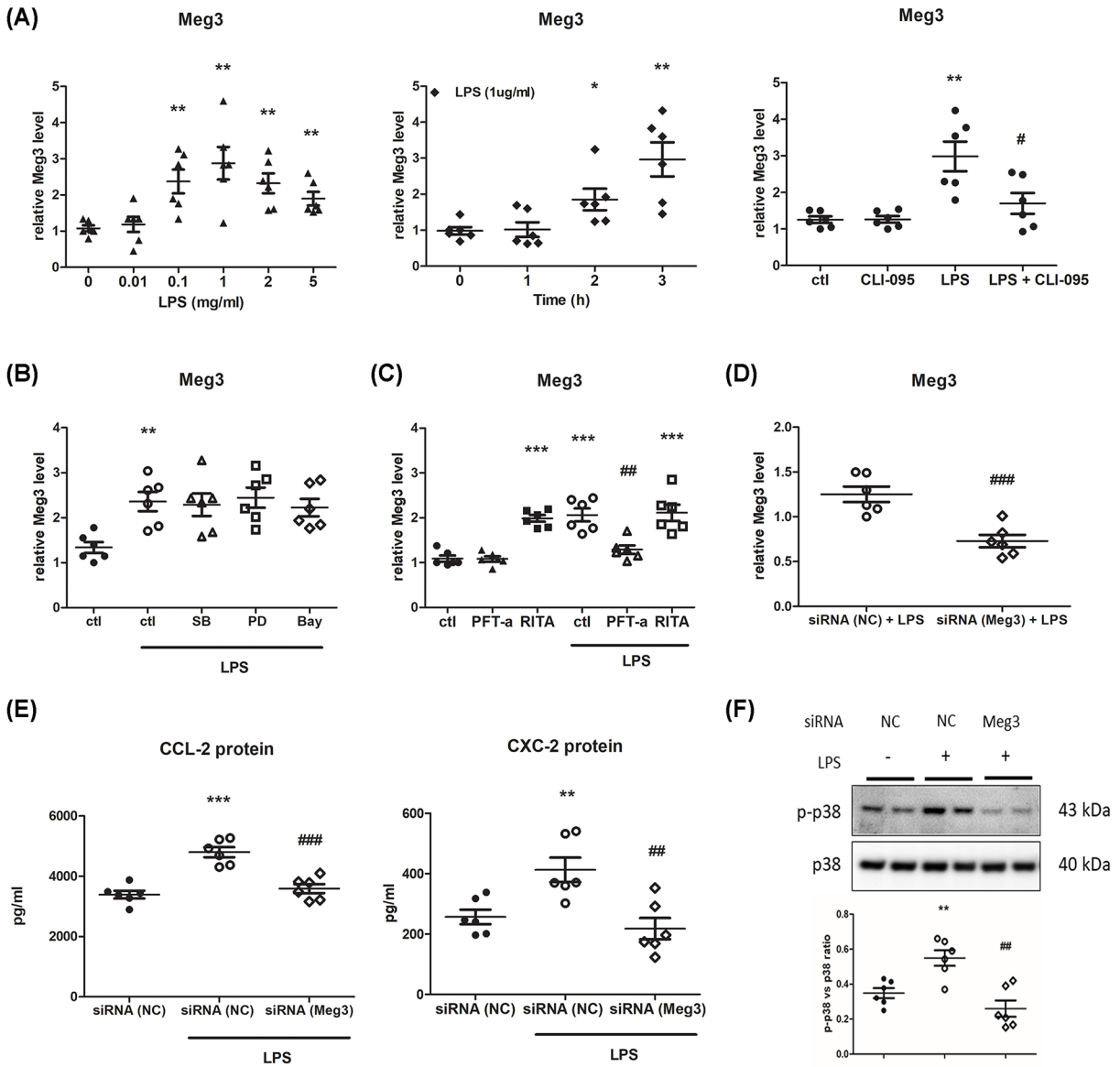

Figure 5. Meg3 mediates TLR4-driven inflammatory responses in tubular cells

Quantitative real-time PCR shows (**A**) the time- and dose-dependent expression of Meg3 in response to LPS in cultured tubular cells, and the effect of TLR4 inhibitor (CLI-095) on LPS-induced Meg3 expression. (**B**) The effect of p38 MAPK inhibitor SB203580 (SB), ERK MAPK inhibitor PD98059 (PD), and NF-κB inhibitor Bay11-7085 (Bay) on LPS-induced Meg3 expression. (**C**) The effect of p53 inhibitor (PFT- α) and p53 activator (RITA) on LPS-induced Meg3 expression. (**D**) Knockdown efficiency of Meg3 in LPS-treated cells. (**E**) ELISA measurement of CCL-2 and CXCL-2 from culture supernatant of LPS-treated groups. (**F**) Western blotting analyses show phosphorylation level of p38 MAPK and total p38 in different groups and the corresponding quantitative analysis. $^{***}P<0.001$, $^{**}P<0.01$ and $^{*}P<0.05$ vs. 0 h, ctl and siRNA (NC); $^{###}P<0.001$, $^{##}P<0.01$ and $^{#}P<0.05$ vs. ctl/LPS and siRNA (NC)/LPS.

TLR4 is differentially expressed on leukocytes and non-immune cells in the diseased kidney for regulating innate and adaptive immune responses in both acute kidney injury and CKD [29]. Interestingly, previous studies show that TLR4 expression on parenchymal cells plays a dominant role in kidney injury rather than those expressed on myeloid cells [6,30]. Using TLR4 global KO mice, we and others have shown that TLR4 mediates inflammatory responses via the activation of NF-κB signaling in tubular epithelial cells and promotes kidney fibrosis by increasing cellular susceptibility toward TGF-β [8,31]. Herein, we showed for the first time that deletion of tubular TLR4 significantly

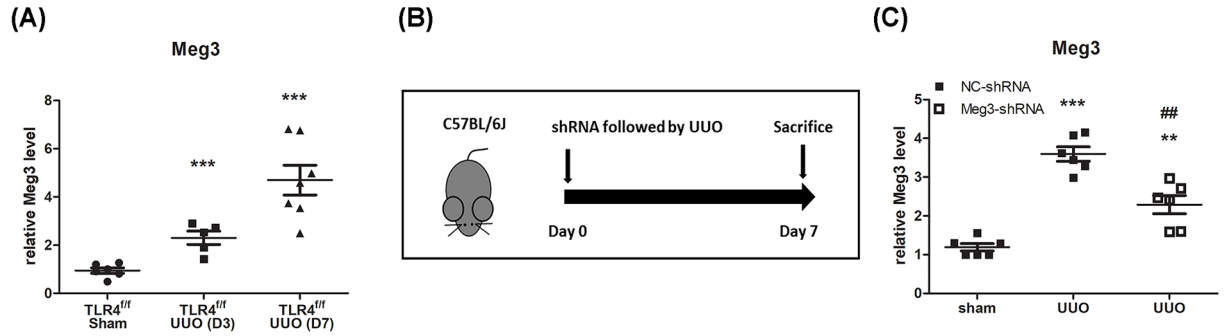

Figure 6. Kidney-specific knockdown of Meg3 in UUO mice

(**A**) Quantitative real-time PCR shows relative expression levels of Meg3 at day 3 and day 7 after UUO. (**B**) The experimental protocol of ultrasound microbubble-mediated shRNA-Meg3 gene knockdown in UUO mice. (**C**) The knockdown efficiency of Meg3 in renal tissues of UUO mice. $^{***}P<0.001$ and $^{**}P<0.01$ vs. sham and TLR4$^{f/f}$ sham mice; $^{\#\#}P<0.01$ vs. NC-shRNA UUO mice.

reduced kidney injury and attenuated collagen deposition in UUO mice although the induction of TLR4 expression was not completely blocked in our conditional tubule-specific KO mice due to the presence of TLR4-expressing macrophages and myofibroblasts. In addition, tubule-specific TLR4 KO mice exhibited suppressed pro-inflammatory CCL-2, CXCL-2 and TNF-α production, accompanied by reduced macrophage accumulation in the obstructed kidney. These findings differed from UUO mice with global TLR4 KO which showed no reduction in macrophage infiltration [31]. This discrepancy may be due to the effect of myeloid TLR4 on macrophage M1/M2 polarization as demonstrated by our previous study [32], absence of myeloid TLR4 led to a shift of infiltrating macrophage from M1 to M2 phenotype in anti-GBM glomerulonephritis model. However, our study indicates that activation of TLR4 signaling in tubular epithelial cells may be the key driver of chronic inflammation in kidney fibrosis, which is consistent with the finding from acute renal ischemia–reperfusion injury on chimeric TLR4 mice [6]. Of note, deletion of tubular TLR4 also reduced accumulation of α-SMA expressing myofibroblasts after UUO whereas comparable myofibroblast activation was shown in the global TLR4 KO model. The existence of EMT in kidney fibrosis is still under debate, but it does not rule out a role of TLR4 in this process. It has been reported that TLR4 regulates EMT in intestinal epithelial cells and contributes to colonic fibrosis [33]. LPS induces EMT in human alveolar type II epithelial cells via up-regulation of TLR4. Thus, our results highlight a prominent role of tubular TLR4 signaling in orchestrating kidney inflammation that leads to EMT and fibrosis.

LncRNAs have emerged as important regulators of gene expression in the innate immune response and many of them are located in close proximity to immune responsive genes [34]. Through transcriptomic analysis, we successfully identified 14 differentially expressed lncRNAs involved in UUO-induced TLR4 signaling. Among these, Meg3 was significantly down-regulated in tubule-specific TLR4 KO mice in response to UUO. Meg3 is a maternally expressed imprinted gene located at the DLK1-Gtl2 locus on mouse chromosome 12 and its human ortholog, MEG3, is located on human chromosome 14q [35]. It is a tumor suppressor that inhibits the proliferation, migration, and invasion of cancer cells [36]. Meg3 also promotes oxidative stress and inflammation in non-cancer cells [37–39]. However, there are other studies showing a protective role of Meg3 against inflammation [40,41]. Here, we showed that up-regulation of Meg3 in UUO kidneys is detrimental as KO of tubular Meg3 suppressed LPS-induced p38 MAPK activation and CCL-2 and CXCL-2 chemokine production. Kidney-specific KO of Meg3 alleviated tubular injury and macrophage infiltration and reduced subsequent kidney fibrosis in UUO mice. In fact, previous studies have suggested a role of Meg3 in the development and progression of diabetic nephropathy. Meg3 was elevated in serum from patients with DN and its expression was correlated with the stage of kidney disease [42]. By acting as a sponge for miR-181a in mesangial cells, Meg3 promoted inflammatory responses and fibrosis in the progression of DN [43]. Besides, Meg3 contributed to podocyte injury by increasing the expression of mitochondrial fission protein Drp1 [44]. Although Meg3 has been implicated in DN, the present study provides evidence for a pathogenic role of Meg3 in tubular inflammation, and most importantly, suggests the involvement of this lncRNA in the regulation of TLR4-driven inflammatory responses during kidney injury.

Accumulating data suggest that lncRNAs serve as an important regulator in TLR4 signaling, including lincRNA-Cox2 and lncRNA NKILA by modulating the expression of inflammatory genes and signaling pathways [45,46]. Our study revealed that knockdown of Meg3 reduced LPS-induced phosphorylation of p38 MAPK in tubular

Clinical Science (2023) **137** 317–331
https://doi.org/10.1042/CS20220537

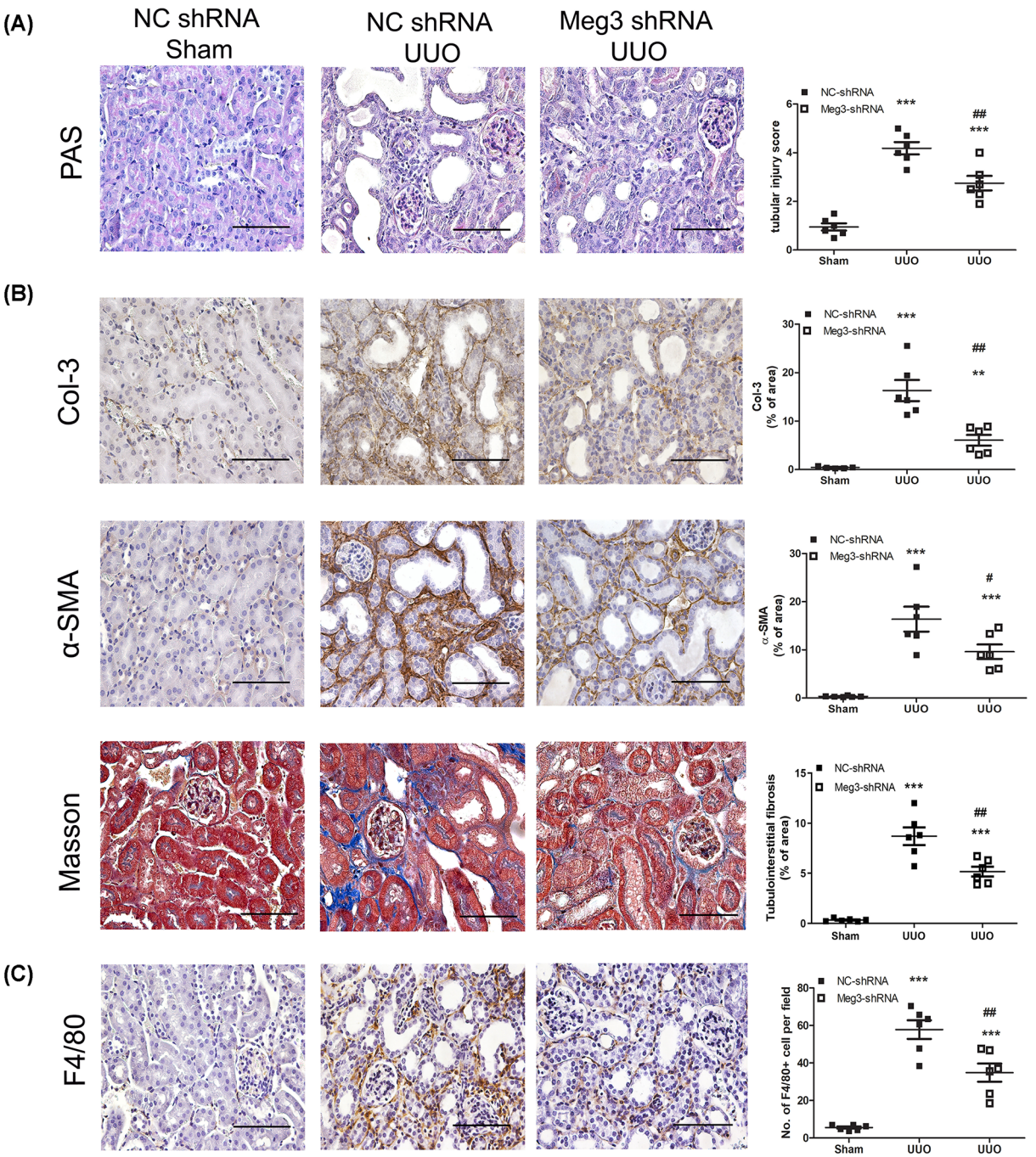

Figure 7. Knockdown of Meg3 by shRNA attenuates kidney fibrosis in UUO mice

(**A**) Representative PAS staining of renal tissues in NC-shRNA sham mice, NC-shRNA UUO mice and Meg3-shRNA UUO mice and quantitative analysis; bar = 100 μm. (**B**) Representative immunohistochemical staining of Col-3, α-SMA and Masson's Trichrome staining in different groups and the corresponding quantitative analysis. (**C**) Representative immunohistochemical staining of F4/80 staining and the corresponding quantitative analysis; bar = 100 μm. ***P<0.001 and **P<0.01 vs. NC-shRNA sham; ##P<0.01 and #P<0.05 vs. NC-shRNA UUO mice (n=7 in each group).

cells. The p38 MAPK signaling pathway plays a vital role in kidney inflammation, apoptosis and fibrosis [47]. Phosphorylation of p38 MAPK is prominent in tubular epithelial cells from various kidney diseases including UUO [48]. Hence, Meg3 regulated the TLR4-induced tubular inflammation and activated the p38 MAPK signaling, resulting in the development of tubulointerstitial fibrosis. Besides, we found that LPS-induced Meg3 expression was mediated by

the up-regulation of p53 in tubular epithelial cells. In the UUO model, p53 could mediate cell cycle arrest, promote EMT and fibrogenesis [39] by activating the transcriptional activities of target genes [49]. Taken together, Meg3 may act as a mediator/regulator of TLR4-induced inflammation, p38 MAPK, and p53-activated pathways.

In summary, this study reveals a prominent role of tubular TLR4 signaling in the development and progression of UUO-induced kidney inflammation and fibrosis. Meg3 mediates TLR4-induced kidney inflammation in both tubular epithelial cells and the UUO kidney via activation of p38 MAPK signaling. Therefore, Meg3 is a novel potential target for CKD.

Clinical perspectives

- Chronic kidney disease (CKD) is a public health problem affecting 10–15% of the world's population. How kidney inflammation contributes to the progression of CKD is not fully understood.
- We identified lncRNA Meg3 as a novel regulator of TLR4-driven inflammatory responses and further generated a tubule-specific TLR4 KO mouse to show the regulatory mechanisms of how kidney tubular TLR4 expression contributed to kidney inflammation and fibrosis.
- We have substantiated a proinflammatory role of lncRNA Meg3 in CKD and suggested a novel regulatory pathway in TLR4-driven inflammatory responses in kidney tubular epithelial cells. Targeting lncRNA Meg3 could become a therapeutic strategy for CKD.

Data Availability

The data underlying this article are available in the article and from the corresponding author upon reasonable requests.

Competing Interests

The authors declare that there are no competing interests associated with the manuscript.

Funding

This work was supported by the Research Grants Council of Hong Kong, Collaborative Research Fund [grant number C7018-16G] and General Research Fund [grant number 17108719 and 17118720].

CRediT Author Contribution

Wai Han Yiu: Conceptualization, Formal analysis, Investigation, Methodology, Writing—original draft. **Sarah W.Y. Lok:** Data curation, Formal analysis, Investigation. **Rui Xue:** Data curation, Formal analysis, Investigation. **Jiaoyi Chen:** Formal analysis, Writing—review & editing. **Kar Neng Lai:** Writing—review & editing. **Hui Yao Lan:** Writing—review & editing. **Sydney C.W. Tang:** Resources, Supervision, Funding acquisition, Project administration, Writing—review & editing.

Acknowledgements

We would like to thank the philanthropic donations from Dr. Rita T Liu SBS of L & T Charitable Foundation Ltd. & Bingei Family of Indo Café, Mr. Winston Leung, Mr. K.K. Chan, Ms. Siu Suet Lau and an Endowment Fund established at the University of Hong Kong for the Yu Professorship in Nephrology awarded to SCWT. We also thank Dr. Xiao Ru Huang from Department of Medicine and Therapeutics, and Li Ka Shing Institute of Health Sciences, the Chinese University of Hong Kong for her contribution to the technical support and advice on the project.

Abbreviations

CDK, chronic kidney disease; DAMP, damage-associated molecular pattern; DEG, differentially expressed gene; DN, diabetic nephropathy; EMT, epithelial–mesenchymal transition; GO, gene ontology; IRI, ischemia-reperfusion injury; KEGG, Kyoto Encyclopedia of Genes and Genomes; KO, knockout; lncRNA, long noncoding RNA; LPS, lipopolysaccharide; Meg3, maternally expressed gene 3; PAMP, pathogen-associated molecular pattern; PAS, periodic acid–Schiff; TLR4, Toll-like receptor 4; UUO, unilateral ureteral obstruction.

Clinical Science (2023) **137** 317–331
https://doi.org/10.1042/CS20220537

References

1 Fu, Y., Xiang, Y., Li, H., Chen, A. and Dong, Z. (2022) Inflammation in kidney repair: mechanism and therapeutic potential. *Pharmacol. Ther.* **237**, , 108240, https://doi.org/10.1016/j.pharmthera.2022.108240

2 Gluba, A., Banach, M., Hannam, S., Mikhailidis, D.P. et al. (2010) The role of Toll-like receptors in renal diseases. *Nat. Rev. Nephrol.* **6**, 224–235, https://doi.org/10.1038/nrneph.2010.16

3 Yiu, W.H., Lin, M. and Tang, S.C. (2014) Toll-like receptor activation: from renal inflammation to fibrosis. *Kidney Int. Suppl. (2011)* **4**, 20–25, https://doi.org/10.1038/kisup.2014.5

4 Liu, B., Yang, Y., Dai, J., Medzhitov, R. et al. (2006) TLR4 up-regulation at protein or gene level is pathogenic for lupus-like autoimmune disease. *J. Immunol.* **177**, 6880–6888, https://doi.org/10.4049/jimmunol.177.10.6880

5 Kruger, B., Krick, S., Dhillon, N., Lerner, S.M. et al. (2009) Donor Toll-like receptor 4 contributes to ischemia and reperfusion injury following human kidney transplantation. *Proc. Natl. Acad. Sci. U. S. A.* **106**, 3390–3395, https://doi.org/10.1073/pnas.0810169106

6 Wu, H., Chen, G., Wyburn, K.R., Yin, J. et al. (2007) TLR4 activation mediates kidney ischemia/reperfusion injury. *J. Clin. Invest.* **117**, 2847–2859, https://doi.org/10.1172/JCI31008

7 Verzola, D., Cappuccino, L., D'Amato, E., Villaggio, B. et al. (2014) Enhanced glomerular Toll-like receptor 4 expression and signaling in patients with type 2 diabetic nephropathy and microalbuminuria. *Kidney Int.* **86**, 1229–1243, https://doi.org/10.1038/ki.2014.116

8 Lin, M., Yiu, W.H., Wu, H.J., Chan, L.Y. et al. (2012) Toll-like receptor 4 promotes tubular inflammation in diabetic nephropathy. *J. Am. Soc. Nephrol.* **23**, 86–102, https://doi.org/10.1681/ASN.2010111210

9 Grabulosa, C.C., Manfredi, S.R., Canziani, M.E., Quinto, B.M.R. et al. (2018) Chronic kidney disease induces inflammation by increasing Toll-like receptor-4, cytokine and cathelicidin expression in neutrophils and monocytes. *Exp. Cell. Res.* **365**, 157–162, https://doi.org/10.1016/j.yexcr.2018.02.022

10 Anders, H.J. and Schlondorff, D. (2007) Toll-like receptors: emerging concepts in kidney disease. *Curr. Opin. Nephrol. Hypertens.* **16**, 177–183, https://doi.org/10.1097/MNH.0b013e32803fb767

11 Song, J., Kim, D., Han, J., Kim, Y. et al. (2015) PBMC and exosome-derived Hotair is a critical regulator and potent marker for rheumatoid arthritis. *Clin. Exp. Med.* **15**, 121–126, https://doi.org/10.1007/s10238-013-0271-4

12 Sun, C., Fu, Y., Gu, X., Xi, X. et al. (2020) Macrophage-enriched lncRNA RAPIA: a novel therapeutic target for atherosclerosis. *Arterioscler. Thromb. Vasc. Biol.* **40**, 1464–1478, https://doi.org/10.1161/ATVBAHA.119.313749

13 Sathishkumar, C., Prabu, P., Mohan, V. and Balasubramanyam, M. (2018) Linking a role of lncRNAs (long non-coding RNAs) with insulin resistance, accelerated senescence, and inflammation in patients with type 2 diabetes. *Hum. Genomics* **12**, 41, https://doi.org/10.1186/s40246-018-0173-3

14 Xia, W., He, Y., Gan, Y., Zhang, B. et al. (2021) Long non-coding RNA: an emerging contributor and potential therapeutic target in renal fibrosis. *Front. Genet.* **12**, 682904, https://doi.org/10.3389/fgene.2021.682904

15 Feng, M., Tang, P.M., Huang, X.R., Sun, S.F. et al. (2018) TGF-beta mediates renal fibrosis via the Smad3-Erbb4-IR long noncoding RNA axis. *Mol. Ther.* **26**, 148–161, https://doi.org/10.1016/j.ymthe.2017.09.024

16 Li, L., Xu, L., Wen, S., Yang, Y. et al. (2020) The effect of lncRNA-ARAP1-AS2/ARAP1 on high glucose-induced cytoskeleton rearrangement and epithelial-mesenchymal transition in human renal tubular epithelial cells. *J. Cell. Physiol.* **235**, 5787–5795, https://doi.org/10.1002/jcp.29512

17 Zhou, J. and Jiang, H. (2019) Livin is involved in TGF-beta1-induced renal tubular epithelial–mesenchymal transition through lncRNA-ATB. *Ann. Transl. Med.* **7**, 463, https://doi.org/10.21037/atm.2019.08.29

18 Xie, Y. and Wei, Y. (2021) A novel regulatory player in the innate immune system: long non-coding RNAs. *Int. J. Mol. Sci.* **22**, 9535, https://doi.org/10.3390/ijms22179535

19 Wang, P., Xue, Y., Han, Y., Lin, L. et al. (2014) The STAT3-binding long noncoding RNA lnc-DC controls human dendritic cell differentiation. *Science* **344**, 310–313, https://doi.org/10.1126/science.1251456

20 Ye, Y., Xu, Y., Lai, Y., He, W. et al. (2018) Long non-coding RNA cox-2 prevents immune evasion and metastasis of hepatocellular carcinoma by altering M1/M2 macrophage polarization. *J. Cell. Biochem.* **119**, 2951–2963, https://doi.org/10.1002/jcb.26509

21 Chen, M.T., Lin, H.S., Shen, C., Ma, Y.N. et al. (2015) PU.1-regulated long noncoding RNA lnc-MC controls human monocyte/macrophage differentiation through interaction with microRNA 199a-5p. *Mol. Cell. Biol.* **35**, 3212–3224, https://doi.org/10.1128/MCB.00429-15

22 Statello, L., Guo, C.J., Chen, L.L. and Huarte, M. (2021) Gene regulation by long non-coding RNAs and its biological functions. *Nat. Rev. Mol. Cell Biol.* **22**, 96–118, https://doi.org/10.1038/s41580-020-00315-9

23 Yiu, W.H., Li, Y., Lok, S.W.Y., Chan, K.W. et al. (2021) Protective role of kallistatin in renal fibrosis via modulation of Wnt/beta-catenin signaling. *Clin. Sci. (Lond.)* **135**, 429–446, https://doi.org/10.1042/CS20201161

24 Yiu, W.H., Wong, D.W., Wu, H.J., Li, R.X. et al. (2016) Kallistatin protects against diabetic nephropathy in db/db mice by suppressing AGE-RAGE-induced oxidative stress. *Kidney Int.* **89**, 386–398, https://doi.org/10.1038/ki.2015.331

25 Lin, M., Yiu, W.H., Li, R.X., Wu, H.J. et al. (2013) The TLR4 antagonist CRX-526 protects against advanced diabetic nephropathy. *Kidney Int.* **83**, 887–900, https://doi.org/10.1038/ki.2013.11

26 Andrade-Oliveira, V., Foresto-Neto, O., Watanabe, I.K.M., Zatz, R. et al. (2019) Inflammation in renal diseases: new and old players. *Front. Pharmacol.* **10**, 1192, https://doi.org/10.3389/fphar.2019.01192

27 Campbell, M.T., Hile, K.L., Zhang, H., Asanuma, H. et al. (2011) Toll-like receptor 4: a novel signaling pathway during renal fibrogenesis. *J. Surg. Res.* **168**, e61–e69, https://doi.org/10.1016/j.jss.2009.09.053

28 Jialal, I., Major, A.M. and Devaraj, S. (2014) Global Toll-like receptor 4 knockout results in decreased renal inflammation, fibrosis and podocytopathy. *J. Diabetes Complications* **28**, 755–761, https://doi.org/10.1016/j.jdiacomp.2014.07.003

29 Cunningham, P.N., Wang, Y., Guo, R., He, G. et al. (2004) Role of Toll-like receptor 4 in endotoxin-induced acute renal failure. *J. Immunol.* **172**, 2629–2635, https://doi.org/10.4049/jimmunol.172.4.2629
30 Zhang, B., Ramesh, G., Uematsu, S., Akira, S. et al. (2008) TLR4 signaling mediates inflammation and tissue injury in nephrotoxicity. *J. Am. Soc. Nephrol.* **19**, 923–932, https://doi.org/10.1681/ASN.2007090982
31 Pulskens, W.P., Rampanelli, E., Teske, G.J., Butter, L.M. et al. (2010) TLR4 promotes fibrosis but attenuates tubular damage in progressive renal injury. *J. Am. Soc. Nephrol.* **21**, 1299–1308, https://doi.org/10.1681/ASN.2009070722
32 Yang, F., Chen, J., Huang, X.R., Yiu, W.H. et al. (2021) Regulatory role and mechanisms of myeloid TLR4 in anti-GBM glomerulonephritis. *Cell. Mol. Life Sci.* **78**, 6721–6734, https://doi.org/10.1007/s00018-021-03936-1
33 Jun, Y.K., Kwon, S.H., Yoon, H.T., Park, H. et al. (2020) Toll-like receptor 4 regulates intestinal fibrosis via cytokine expression and epithelial–mesenchymal transition. *Sci. Rep.* **10**, 19867, https://doi.org/10.1038/s41598-020-76880-y
34 Aune, T.M. and Spurlock, III, C.F. (2016) Long non-coding RNAs in innate and adaptive immunity. *Virus Res.* **212**, 146–160, https://doi.org/10.1016/j.virusres.2015.07.003
35 Miyoshi, N., Wagatsuma, H., Wakana, S., Shiroishi, T. et al. (2000) Identification of an imprinted gene, Meg3/Gtl2 and its human homologue MEG3, first mapped on mouse distal chromosome 12 and human chromosome 14q. *Genes Cells* **5**, 211–220, https://doi.org/10.1046/j.1365-2443.2000.00320.x
36 Ghafouri-Fard, S. and Taheri, M. (2019) Maternally expressed gene 3 (MEG3): a tumor suppressor long non coding RNA. *Biomed. Pharmacother.* **118**, 109129, https://doi.org/10.1016/j.biopha.2019.109129
37 Li, J., Bai, J., Tuerdi, N. and Liu, K. (2022) Long non-coding RNA MEG3 promotes tumor necrosis factor-alpha induced oxidative stress and apoptosis in interstitial cells of cajal via targeting the microRNA-21 /I-kappa-B-kinase beta axis. *Bioengineered* **13**, 8676–8688, https://doi.org/10.1080/21655979.2022.2054501
38 Dong, J., Xia, R., Zhang, Z. and Xu, C. (2021) lncRNA MEG3 aggravated neuropathic pain and astrocyte overaction through mediating miR-130a-5p/CXCL12/CXCR4 axis. *Aging (Albany NY)* **13**, 23004–23019, https://doi.org/10.18632/aging.203592
39 Liu, L., Zhang, P., Bai, M., He, L. et al. (2019) p53 upregulated by HIF-1alpha promotes hypoxia-induced G2/M arrest and renal fibrosis in vitro and in vivo. *J. Mol. Cell Biol.* **11**, 371–382, https://doi.org/10.1093/jmcb/mjy042
40 Zou, D., Liu, L., Zeng, Y., Wang, H. et al. (2022) LncRNA MEG3 up-regulates SIRT6 by ubiquitinating EZH2 and alleviates nonalcoholic fatty liver disease. *Cell Death Discov.* **8**, 103, https://doi.org/10.1038/s41420-022-00889-7
41 Huang, Y., Chen, D., Yan, Z., Zhan, J. et al. (2021) LncRNA MEG3 protects chondrocytes from IL-1 beta-induced inflammation via regulating miR-9-5p/KLF4 axis. *Front. Physiol.* **12**, 617654, https://doi.org/10.3389/fphys.2021.617654
42 Li, J., Jiang, X., Duan, L. and Wang, W. (2019) Long non-coding RNA MEG3 impacts diabetic nephropathy progression through sponging miR-145. *Am. J. Transl. Res.* **11**, 6691–6698
43 Zha, F., Qu, X., Tang, B., Li, J. et al. (2019) Long non-coding RNA MEG3 promotes fibrosis and inflammatory response in diabetic nephropathy via miR-181a/Egr-1/TLR4 axis. *Aging (Albany NY)* **11**, 3716–3730, https://doi.org/10.18632/aging.102011
44 Deng, Q., Wen, R., Liu, S., Chen, X. et al. (2020) Increased long noncoding RNA maternally expressed gene 3 contributes to podocyte injury induced by high glucose through regulation of mitochondrial fission. *Cell Death Dis.* **11**, 814, https://doi.org/10.1038/s41419-020-03022-7
45 Carpenter, S., Aiello, D., Atianand, M.K., Ricci, E.P. et al. (2013) A long noncoding RNA mediates both activation and repression of immune response genes. *Science* **341**, 789–792, https://doi.org/10.1126/science.1240925
46 Liu, B., Sun, L., Liu, Q., Gong, C. et al. (2015) A cytoplasmic NF-kappaB interacting long noncoding RNA blocks IkappaB phosphorylation and suppresses breast cancer metastasis. *Cancer Cell* **27**, 370–381, https://doi.org/10.1016/j.ccell.2015.02.004
47 Stambe, C., Atkins, R.C., Tesch, G.H., Masaki, T. et al. (2004) The role of p38alpha mitogen-activated protein kinase activation in renal fibrosis. *J. Am. Soc. Nephrol.* **15**, 370–379, https://doi.org/10.1097/01.ASN.0000109669.23650.56
48 Ma, F.Y., Tesch, G.H. and Nikolic-Paterson, D.J. (2014) ASK1/p38 signaling in renal tubular epithelial cells promotes renal fibrosis in the mouse obstructed kidney. *Am. J. Physiol. Renal. Physiol.* **307**, F1263–F1273, https://doi.org/10.1152/ajprenal.00211.2014
49 Zhou, Y., Zhong, Y., Wang, Y., Zhang, X. et al. (2007) Activation of p53 by MEG3 non-coding RNA. *J. Biol. Chem.* **282**, 24731–24742, https://doi.org/10.1074/jbc.M702029200

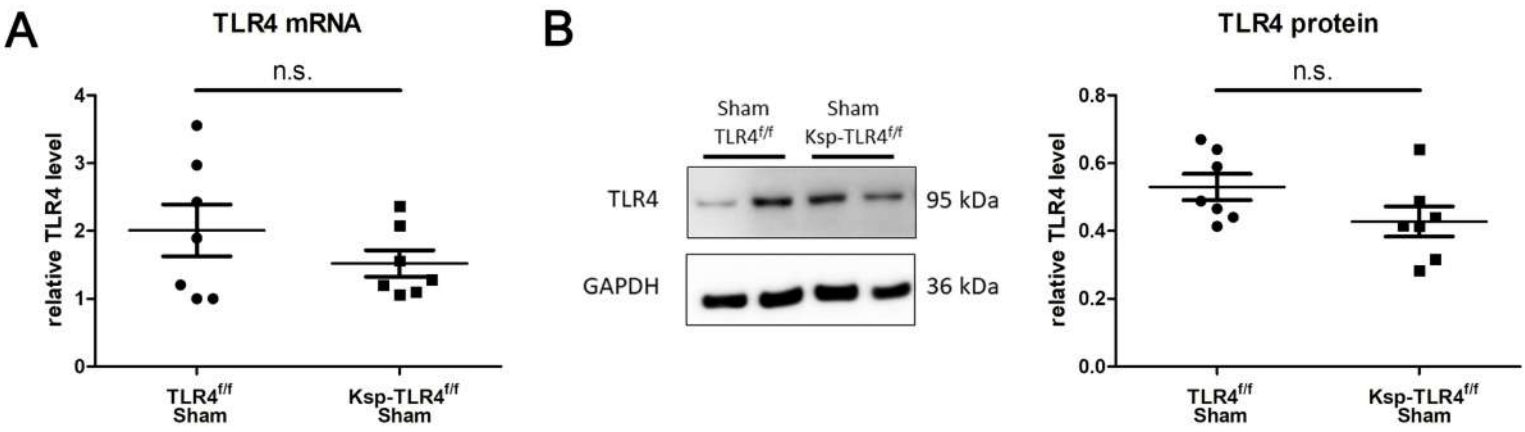
A
TLR4 mRNA
n.s.
relative TLR4 level
4
3
2
1
0
TLR4f/f Sham
Ksp-TLR4f/f Sham
B
Sham TLR4f/f
Sham Ksp-TLR4f/f
TLR4
95 kDa
GAPDH
36 kDa
TLR4 protein
n.s.
relative TLR4 level
0.8
0.6
0.4
0.2
0.0
TLR4f/f Sham
Ksp-TLR4f/f Sham

Figure S1. Renal TLR4 expression in tubule-specific TLR4 knockout mice under normal physiologic conditions (**A**) Real-time analysis of TLR4 mRNA expression in $TLR4^{f/f}$ sham mice and Ksp-$TLR4^{f/f}$ sham mice. (**B**) TLR4 protein expression as determined by Western blot analysis. (n=7 in each group)